energy&fuels

ARTICLE

pubs.acs.org/EF

Quality Prediction from Hydroprocessing through Infrared Spectroscopy (IR)

Jorge A. Orrego-Ruiz,[†,‡,*] Enrique Mejía-Ospino,[‡] Lante Carbognani,[†] Francisco López-Linares,[†] and Pedro Pereira-Almao[†]

[†]Department of Chemical and Petroleum Engineering, Schulich School of Engineering, University of Calgary, Calgary, AB T2N 1N4, Canada

[‡]Laboratorio de Espectroscopía Atómica y Molecular, Escuela de Química, Universidad Industrial de Santander, Bucaramanga, A.A. 678, Colombia

ABSTRACT: A fast, reliable, and inexpensive way to monitor the quality of hydroprocessed products from a heavy bitumen distillate is presented in this work. Predictive models for density, nitrogen and sulfur contents, and weight percentage of lumped products, in this case, the distillation cuts IBP−235, 235−280, 280−343, and 343+ °C, were obtained through Fourier transform infrared spectroscopy (FTIR) and partial least squares regression (PLS-R). In addition, two structural parameters also derived from FTIR spectroscopy are proposed for chemical understanding of the former process. Two sets of hydroprocessing experimental runs were conducted under various operating conditions to evaluate the nature of the hydrocarbon (HC) products from two different catalysts. The statistic validation of the models demonstrated the capability to predict accurately physicochemical properties of a wide range distillation cut. Simplicity and accuracy make FTIR-PLS a promising tool for online estimation of process conversion as well as products properties at pilot scale and even in refinery facilities.

INTRODUCTION

The demand for high value petroleum products such as middle distillates, gasoline, and lube oil is increasing, while the demand for low value products such as fuel oil and residua based products is decreasing.[1] Upgrading is generally defined as any fractionation or chemical treatment of bitumen or heavy oil that increases its value.[2] Hydroprocessing, as an upgrading option, is a thermal catalytic process comprising the incorporation of hydrogen to the feed to increase the hydrogen to carbon ratio and reduce the formation of coke.[3] Hydroprocessing reactions can be both molecularly destructive and nondestructive. Destructive hydroprocessing such as hydrocracking is the conversion of compounds with high molecular weight into lower molecular weight compounds. Carbon−carbon bonds break and then are saturated with hydrogen. Nondestructive hydroprocessing consists in hydrogenation reactions that improve oil quality by removing certain contaminants such as sulfur, nitrogen, and metals.[4] Quality control of this process is normally performed by measuring density, simulated distillation (SIMDIS), and nitrogen and sulfur contents of the produced fractions. However, these analyses are limited by the availability of specialized equipments and require time spans that normally prevent decision-making in real time operation. Measuring these properties for ten samples requires a time span of about one day, provided all the involved analytical systems are running 24/7.

If during hydroprocessing the carbon−carbon bonds break and unsaturated bonds are saturated, FTIR spectroscopy, which is a fast, well established, inexpensive, and available technique for the most of the analytic laboratories, should be able to detect the molecular changes on the feed. However, this is not a straightforward situation when heavy distillates such as vacuum gas oil (VGO) or fractions containing substantial amounts of heavy hydrocarbons are studied. Normally, an infrared spectrum is selected for qualitative analysis, considering the presence or absence of bands that are usually assigned to particular functional groups. Nevertheless, quantitative analyses following traditional procedures through the Beer−Lambert law have several problems associated with the sensitivity to temperature changes and nonlinear detector response, which causes baseline drift, and therefore poor spectral repeatability.[6] It is also complicated to follow these reactions by the variation of one specific IR band, because many functional groups are involved. Hence, multivariate analysis (chemometry) is desirable. IR spectroscopy has received an important impulse by chemometry.[5] The success of chemometric tools, such as partial least squares (PLS), lies in the ability to extract information from data for further association with gross properties of samples, making IR methodologies of real use in many complex situations. Thus, IR spectroscopy can be employed as an analytical aid to decision-making during critical operations.[7]

Sample collection and accessories such as transmittance, attenuated total reflectance (ATR), diffuse reflectance (DRIFT), specular reflectance, and photoacoustic spectroscopy (PAS) have been developed to collect spectra as solids, liquids, vapors, and aqueous solutions from the same FTIR instrument. Solid samples are mostly analyzed by DRIFT and PAS, liquid and aqueous samples by ATR, and gases by transmittance.[8] However, transmittance is the traditional accessory to record IR spectra independently of physical state of samples. Because of scattering and reflectance of radiation, acquiring spectra from liquid or solid samples by transmittance can render a variable baseline. If this

Received: October 12, 2011
Revised: November 17, 2011
Published: November 18, 2011

dx.doi.org/10.1021/ef201562j | *Energy Fuels* 2012, 26, 586–593

problem is not overcome, assuring spectral repeatability and performing multivariate analyses would be impossible.

In the present work, we describe a novel way to monitor the quality of converted products from hydroprocessing of heavy bitumen distillate. Predictive models for density, nitrogen and sulfur contents, and weight percentage of IBP−235, 235−280, 280−343, 343+ °C distillation cuts were obtained through IR and PLS-R. In addition, two structural parameters from IR are proposed for chemically understanding the hydroprocessing of heavy distillates. Two sets of experimental runs were conducted under various operating conditions to study the upgrading products using two different catalysts. The statistical validation parameters demonstrated the capability of this methodology to predict accurately physicochemical properties in a wide range of hydroconversion.

EXPERIMENTAL SECTION

Solvents, Samples, and Gases. Toluene (spectrophotometric grade), methylene chloride, *n*-heptane, and tetrahydrofuran (THF), all (HPLC grade) from Sigma-Aldrich, were used as received. H_2, air, and N_2 of UHP grade were purchased from Praxair Canada. The feedstock for hydroconversion was a heavy distillate derived from bitumen from the province of Alberta, Canada. This material contains 64.51% w/w boiling above 343 °C, and its N and S contents were respectively 0.14 and 2.76% w/w. A total of 130 samples were produced in two sequences. A detail of the hydroprocessing unit has been published elsewhere.[2,9] The upgraded products were orange to yellow low viscous liquid full gas oils, that is, distillates spanning from naphtha fractions up to VGO.

Standard Hydrocarbons. The following standard hydrocarbons were used as received for reference IR spectra determination: 1,2,3, 4-tetrahydronaphtalene (Sigma-Aldrich P/N 429325-1L, 99% purity, CAS 119-64-2), decahydronaphtalene (Sigma-Aldrich P/N D251-500ML, 98% purity, CAS 91-17-8), 1-methylnaphthalene (Sigma-Aldrich P/N M56808-500G, 95% purity, CAS 90-12-0), fluorene (Aldrich P/N 12,833-3, 98% purity, CAS 86-73-7), pyrene (Aldrich P/N 185515-25G, 98% purity, CAS 129-00-0), phenanthrene (Aldrich P/N 11409-500G, 98% purity, CAS 85-01-8), chrysene (Fluka P/N 35754, 98.3% purity, CAS 218-01-9), coronene (Aldrich P/N C84801-100MG, 97% purity, CAS 191-07-1), methylcyclohexane (Sigma-Aldrich P/N M37889-500ML, 99% purity, CAS 108-87-2), *n*-propylbenzene (Sigma-Aldrich P/N 82119-100ML, ≥ 99,0% purity, CAS 103-65-1), and 2,2, 4-trimethylpentane (Sigma-Aldrich P/N 258776-2L, ≥ 99% purity, CAS 540-84-1)

Product Characterization. The products distribution was analyzed by simulated distillation carried out in a gas chromatograph from Agilent Technologies modified by Separation Systems, Inc. The cuts were establish as naphtha (IBP−235 °C), kero (235−280 °C), light gas oil (280−343 °C), and the "residue" which comprises VGO fractions (>343 °C). To estimate the amount of residue at 343+ °C, ASTM D7169-2005, as described by Carbognani et.al,[10] was used. Conversions of products, as defined in eq 1, are presented in Figure 1.

$$\%\ \mathrm{wt}_{\mathrm{conversion}} = [(\%\ \mathrm{wt\ IBP} > 343^{\circ}\mathrm{C}_{\mathrm{feedstock}} - \%\ \mathrm{wt\ IBP} > 343^{\circ}\mathrm{C}_{\mathrm{product}})/(\%\ \mathrm{wt\ IBP} > 343^{\circ}\mathrm{C}_{\mathrm{feedstock}})] \times 100 \quad (1)$$

All products were characterized by measuring the density following a procedure proposed by Carbognani et al.[11] Selected samples were characterized by measuring elemental nitrogen and sulfur content with an Antek 9000 analyzer. Toluene sample solutions ca. 10% (w/w) were injected with the provided autosampler (CTC Analytical) and the syringe automatic injector system (Antek 735 plus Antek 740). Calibration

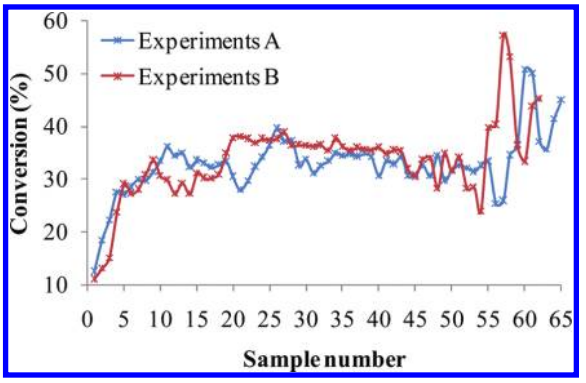

Figure 1. Hydroprocessing yield of sequences A and B.

was performed using heavy gas oil (HGO) as the standard reference material.[12] After the experimental sequences, the changes in conversion were thoroughly reviewed (Figure 1), and 88 samples were chosen to build the predictive models for density, IBP−235, 235−280, 280−343, and 343 + °C distillation cuts, and 39 for nitrogen and sulfur content using FTIR and PLS-R. To further study the mechanisms of reactions involved in this process, 20 L batches of selected samples from sequences A and B were scale-preparative distilled into the physical distillation cuts IBP−235, 235−280, 280−343, and 343+ °C, following the procedure ASTM D 2892-03a[13] and ASTM D 5236-03.[14] The density of each distillation cut was also further measured.

Initially, the operational conditions were modified to simulate the aging of the catalysts and their performance under different temperatures and space velocities. From Figure 1, three regions can be distinguished: (1) start-setting up (1 to 30), (2) aging (31 to 55 for A and 31 to 51 for B), and (3) equilibrium (56 to 65 for A and 52 to 62 for B). Conversion maxima were achieved for products 61 A and 57 B.

Acquisition of FTIR Spectra. FTIR spectra in transmittance mode were recorded on a Nicolet 6700 spectrometer with a spectral resolution of 8 cm^{-1} over the range of 4000−700 cm^{-1} and 16 scans. The spectrometer was equipped with a mercury cadmium telluride (MCT) detector. Each sample was spread over a KBr cell as a film and immediately put inside the chamber to acquire the spectrum. The acquisition time for 16 scans was approximately 30 s. The background was collected for every sample before the analysis in the single-beam mode with the same clean KBr cell (dichloromethane HPLC grade was used for cleaning). Triplicate spectra were acquired for each sample. The spectral files were transformed to ASCII format using the Omnic software, version 7.3 and exported to The Unscrambler software, version X, where the data pretreatment and PLS-R were performed.

Data Pretreatment. All spectra were baseline corrected. This transformation consisted of subtracting the minimum intensity from each of IR intensities (which is to correct baseline respect to offset) and then transforming a sloping baseline into a horizontal baseline (which is linear baseline correction), taking as reference the intensities at 700 and 4000 cm^{-1}. It was performed on all data in a systematic way to avoid subjective influence. After this, the regions 1970−2697 cm^{-1} and 3140−4000 cm^{-1} were eliminated from the spectra. These regions do not offer a particular spectral variability because they do not have bands that can be assigned to functionalities for the studied distillates samples. The remaining spectral intensities were normalized to the sum of all intensities (area normalization). It means that each intensity was divided by the sum of all intensities. Thus, the samples can be compared between them, and their relative intensities can provide information concerning chemical changes associated during hydroprocessing.

Partial Least Squares Regression (PLS-R). PLS-R was used to establish the relationship between IR spectral intensities (*X*-variables)

dx.doi.org/10.1021/ef201562j |*Energy Fuels* 2012, 26, 586–593

and the physicochemical analyses in samples (*Y*-properties). A total of 88 samples were chosen to build the predictive models, which means a total of 244 spectra (three replicates for each sample were recorded); that is, the PLS-R was performed with a higher number of spectra than samples. Forty-four samples were used for calibration of density, IBP−235, 235−280, 280−343, and 343+ °C models, and 44 samples were used for external validation. The construction of nitrogen and sulfur content was performed from 39 samples, from which 29 were used for calibration and 10 were used for external validation. The building of models was done by the variable reduction procedure reported by Orrego-Ruiz et al.,[15] using a cross-validation procedure with 20 segments chosen randomly. The *X*-variables remaining were proved via Martens' Uncertainty Test to evaluate their significance. This test consists in calculating the difference between the regression coefficients (or *B*-coefficient) in a submodel and the regression coefficients for the total model, when cross-validation is used. Under cross-validation, a number of submodels are created. These submodels are based on all the samples that were not kept out in the cross-validation segment. For every submodel, a set of *B*-coefficients (B_i) was calculated. Variations over these submodels are estimated so as to assess the stability of the results.[16] The sum of the squares is taken of the differences in all submodels to get an expression of the variance of the B_i estimate for a variable. With a *t* test, the significance of the estimate of B_i is calculated. Thus, the resulting regression coefficients can be presented with uncertainty limits that correspond to 2 standard deviations. Variables with uncertainty limits that do not cross the zero line are significant variables.[17] The nonsignificant *X*-variables were finally excluded.

RESULTS AND DISCUSSION

Spectra repeatability. It was mandatory to ensure that IR spectral variability was due to structural differences between the samples and not derived from instrumental causes. For that reason, 53 samples from sequence B were used to establish the spectral repeatability. For every sample, three spectra were acquired to calculate the relative standard deviation (RSD) on each IR intensity.[18] Figure 2 shows the average, maximum, and minimum RSD of all IR intensities comprised between 3135 and 2700 cm^{-1} and 1900−700 cm^{-1} where functional groups show spectral contributions. From this figure, the RSD averages were less than 7% (an exception is observed within the range 1850−1650 cm^{-1}). This means that further predictions will have average variations under 7% as long as the intensities comprised in these regions are used. This assured the reliability of the methodology. Something remarkable is that, in the region 3020−2715 cm^{-1}, even the RSD maxima were below to 10%; namely, in this spectral region, all triplicates for all samples had a repeatability minor than 10%.

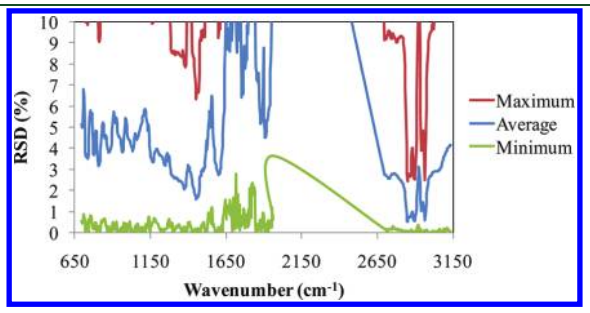

Figure 2. Precision of IR spectra on selected samples.

Partial Least Squares Regression (PLS-R). Before analyzing these results, it is necessary to specify that the errors for Simdist are lower than 1 wt % absolute within the whole distillation range, which are accepted within ASTM D7169 for the distillation ranges defined in this work.[10] Concerning S,N errors with the Antek analyzer, they are routinely less than 3% relative, even though it is always guaranteed that less than 5% relative error is the maximum. The main statistic parameters, together with calibration ranges and the number of samples for calibration and validation, are included in Table 1. Significantly, it was not necessary to exclude any sample as an outlier (except in one model), considering 88 and 39 are non-negligible numbers of samples. It can be appreciated the closeness to 1 for the correlations. These values are associated with the *Y*-variance explained by the *X*-variables and confirm their significances. The lowest values for correlations and slopes (which correspond to the slopes of predicted versus measured plots) were for the models of distillation cuts 235−280 °C and 280−343 °C; something attributed to their small ranges of calibration. Broadly, the samples did not vary so much for these parameters in comparison with those for IBP−235 and 343+ °C, even though it should be also considered that not all the data variance can be explained by linear relationships between *X*-variables and *Y*-properties, and the models themselves have an uncertainty inherited from the starting methodologies and from the spectral repeatability. The offset is the *Y*-intercept in the predicted versus measured plot. This value is relative to the data scale; therefore, it cannot be compared between models. The lower the data scale, as in density, the lower the offset is, while for higher data scales, as determined by sulfur content, the higher the offset is. Nonetheless, as offset is closer to zero, the model is more reliable because predicted values are closer to measured ones. The same can be said regarding the root mean square error (RMSE). This parameter is related to the accuracy of determinations and could

Table 1. Statistic Parameters from the Predictive Models

		calibration range		correlation		slope		offset		RMSE		samples			
property	unit	min	max	cal[a]	val[b]	cal	val	cal	val	cal	val	cal	val	LVs[c]	outliers
density	g/mL	0.816	0.888	0.987	0.977	0.973	1.021	0.022	−0.018	0.0018	0.0023	44	44	8	0
N content	ppm wt	10	408	0.980	0.967	0.960	0.985	3.53	−8.97	18.9	24.0	29	10	10	0
S content	ppm wt	90	2111	0.966	0.971	0.932	1.020	39.5	−20.6	108	103	29	10	10	0
IBP−235 °C	% wt	10.92	40.29	0.977	0.950	0.955	0.964	1.096	0.490	1.241	1.453	44	44	10	0
235−280 °C	% wt	7.97	18.09	0.944	0.868	0.892	0.995	1.345	0.021	0.504	0.381	44	44	7	1
280−343 °C	% wt	15.22	21.6	0.930	0.934	0.864	0.981	2.726	0.289	0.483	0.430	44	44	10	0
343+ °C	% wt	27.60	64.51	0.973	0.948	0.946	0.962	2.305	1.798	1.578	1.510	44	44	8	0

[a] cal: calibration. [b] val: validation. [c] LVs: latent variables.

dx.doi.org/10.1021/ef201562j |*Energy Fuels* 2012, 26, 586–593

be associated with the detection limit. By comparing the RMSE of validation of the distillation ranges with the errors of the initial methods, it can be concluded that the prediction models offer a similar performance to the primary methods.

Now, if the RMSE is higher than the calibration lowest value, then the detection limit is above the minimum calibration value. It was the case for nitrogen and sulfur contents. For these models the RMSE of calibration were 18.9 ppm and 103 ppm, respectively, and their minimum calibration values were 10 ppm and 90 ppm, respectively. It means, if one sample had nitrogen and sulfur contents of 15 ppm and 100 ppm, respectively, the accuracy of these values cannot be assured. So, this methodology must be used carefully when sulfur and nitrogen are present in low concentrations. The model for density had the lower RMSE (with respect to its minimum value of calibration), which may be due to it is a gravimetric method. Figure 3 shows the plot of predicted versus measured validation values for all the models. For every measured value, three values were predicted, which were matched to a linear tendency in a wide validation range and supports the precision of the models.

So far, the results demonstrate that, through one simple IR spectrum, it is possible to predict simultaneously several physicochemical properties of upgraded full gas oils with high reliability, considering the closeness of the correlations to 1 and the low values for the errors in the prediction of external samples (Table 1). Furthermore, this procedure is faster than traditional ones insomuch as acquiring one IR spectrum may take five minutes and once the spectrum is recorded, preprocessing and prediction of all the properties takes five additional minutes. Ten samples can be characterized in one labor hour, unlike routine methodologies that would demand approximately sixteen labor hours (1 day time span). Monetary savings in samples characterization of at least 80% are estimated, considering that labor cost/spectrum acquisition is about 5 USD.

Nevertheless, these predictive models have a limitation. Every time that a new population of samples is analyzed (not included in the original range of calibration), a new modeling process is required. This was one of the motivations to go deeply to understand the relationship between the functional groups detected by IR spectroscopy and *B*-coefficients. Considering that conversion is the most important parameter during hydroprocessing, the predictive model for naphtha fractions (IBP−235 °C) and unconverted feedstock (343+ °C) were deemed important and selected for closer study.

Figure 4 shows the *B*-coefficients obtained for the IBP−235 and 343+ °C models, which are located in three spectral regions. The first one (region I, from 700 to 900 cm^{-1}) comprises almost exclusively aromatics functionalities. Some reports from the literature proposed structural parameters responsible for the condensation grade on aromatic rings for coals and asphaltenes using spectral intensities in this region.[19−21] The second one (region II, from 1350 to 1500 cm^{-1}) contains information for aliphatic groups, by the bands assigned to flexion vibrational modes for CH_3 and CH_2 groups. In the third one (region III, from 2850 to 3050 cm^{-1}) there are attributable signals to stretching modes for CH_3, CH_2, and CH aliphatic bonds and for CH aromatics.

A positive *B*-coefficient indicates a direct relationship between the functional group and the studied property, whereas a negative *B*-coefficient indicates an inverse correlation. Noteworthy, as shown in Figure 4, positive *B*-coefficients for IBP−235 °C are negative in 343+ °C and vice versa. This means that one sample with a high concentration of functional groups with positive *B*-coefficients has higher IBP−235 wt % and lower 343+ °C wt %. It demonstrates how heavy fractions hydroprocessing follows the expected trend of transformation of 343+ °C fractions into lighter fractions. The principal purpose of hydroprocessing is to upgrade the feed through the redistribution of heavy ends (343+ °C) into distillation cuts within the IBP−343 °C range.

Structural Parameters. To understand which functional groups are emerging and which are disappearing during hydroprocessing reactions, the IR spectra of eleven standard hydrocarbons were acquired. Mono-, di-, and polyaromatic structures (tri-, tetra-, and hexa-aromatic rings) as well as aliphatic ones with varying chain length were recorded. First, the aromatic region from 700 to 900 cm^{-1}, which mainly corresponds to out-of-plane wagging of the CH bonds, was considered. Concerning the C_{ar}−H vibrations, the positions of the main bands depend on the number of adjacent hydrogens involved on consecutive carbons, but do not discriminate what type of groups substitute the aromatic ring (alkyls or aryls). The solo, duo, and quarto occur around 892 cm^{-1}, 833 cm^{-1}, and 746 cm^{-1}, respectively.[22] Nonetheless, the peak positions can vary substantially according to the symmetry of the molecule. The lower the symmetry of these species, the intensity is spread out into more bands and vice versa.[23]

In detail, Figure 5a shows three bands at 740, 779, and 802 cm^{-1}, which represent the positive *B*-coefficient for IBP−235 model, matching with mono- and diaromatic bands of studied reference standards. These bands correspond to bending out of plane for C_{ar}−H for mono- or disubstituted aromatic rings, that is, with five and four adjacent hydrogens.

On the other hand, Figure 5b shows the most representative bands from polyaromatic rings at the same wavenumbers corresponding to negative *B*-coefficients. This means the presence of tri- or tetra- fused aromatic rings in hydroprocessed FGO decreases within the IBP−235 cut. The IBP−235 °C fraction comprises mono- and diaromatic rings, while the 343+ °C fraction preferentially contains polyaromatic rings. Chrysene and phenanthrene have duo and quarto around 816 and 755 cm^{-1}, respectively. Pyrene has duo and trio around 841 and 752 cm^{-1}. Even though this molecule has three hydrogens on two of the rings, the higher wavenumber band is more reminiscent of a hydrogen duo.[24] The two bands around 710 cm^{-1} from pyrene and phenanthrene are characteristic of the $\tau_{(CCCC)}$ out-of-plane deformations of the cycles often described as butterfly modes, but in plane, angular deformations of the carbon skeleton.[22] Coronene has a predominant band around 850 cm^{-1} because its hydrogens are duos, being chemically equivalent. This band is slightly shifted from the duo of pyrene.

Furthermore, spectra of the IBP−235 and 343+ °C distillation cuts from both sets of experiments were acquired and compared. Figure 6 includes the 700−900 cm^{-1} spectral region for A and B fractions. Bands within 710−724 cm^{-1} correspond to $-CH_2$ rocking from long alkyl moieties, the remainder correspond to out-of-plane C_{ar}−H bending vibrations. In Figure 6, encased in blue squares are presented the bands at 740, 767, and 806 cm^{-1} whose relative intensities are higher for IBP−235 °C, and in red squares are the regions 705−729 cm^{-1} and 810−900 cm^{-1} where relative intensities are higher for 343+ °C. It allows confirming that 343+ °C fraction is enriched with polyaromatic fused rings. Thus, it is valid, affirming that, during hydroprocessing, polyaromatic rings are hydrogenated toward mono- and diaromatics and long alkyl substituents from heavy fractions are

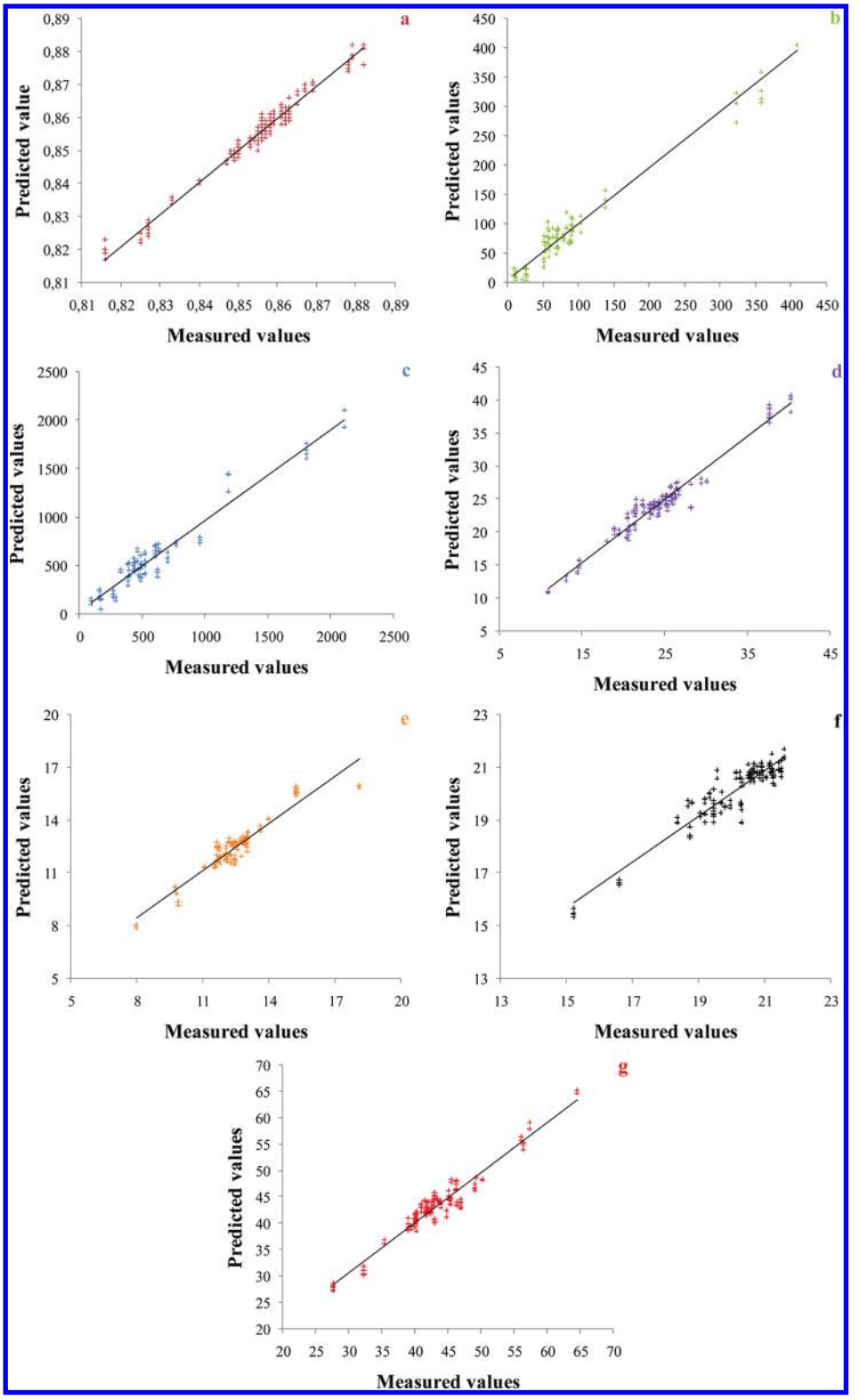

Figure 3. Predictions for validation samples: (a) density, (b) nitrogen content, (c) sulfur content, (d) IBP−235 °C, (e) 235−280 °C, (f) 280−343 °C, and (g) 343+ °C.

cracked into smaller compounds that partition into the pool of lighter compounds (IBP−343 °C) within products.

To reinforce the previous statements and to explain hydroprocessing reaction progress, IR spectra from the most representative samples, the feedstock, and some distillation fractions were band-fitted on the aromatic region. The number and position of the single components used for the fitting procedure were evaluated by visual overlapping, finding a good match between the sum of simulated bands and the spectra. The regression coefficients were above 0.99, employing Gaussian

dx.doi.org/10.1021/ef201562j |*Energy Fuels* 2012, 26, 586–593

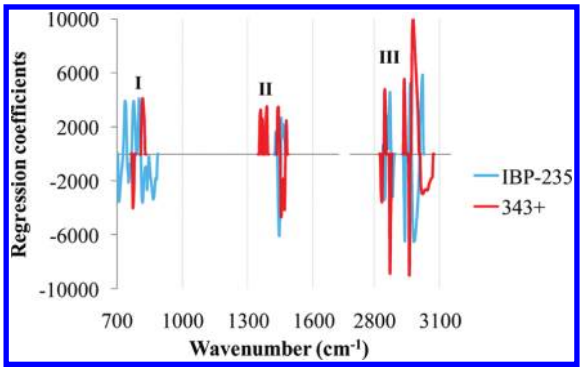

Figure 4. Regression coefficients for IBP−235 and 343+ °C predictive models.

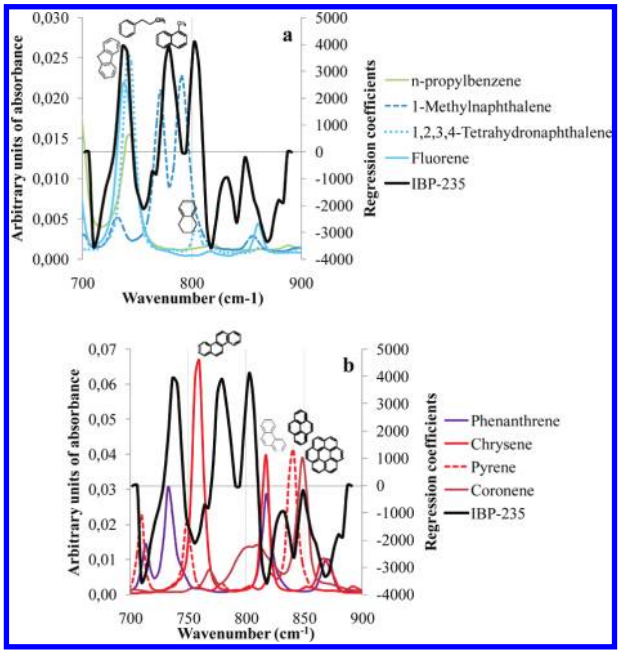

Figure 5. Comparison between IBP−235 model regression coefficients and IR spectra at the spectral region 700−900 cm^{-1} of (a) mono- and diaromatic standard HCs and (b) polyaromatic standard HCs.

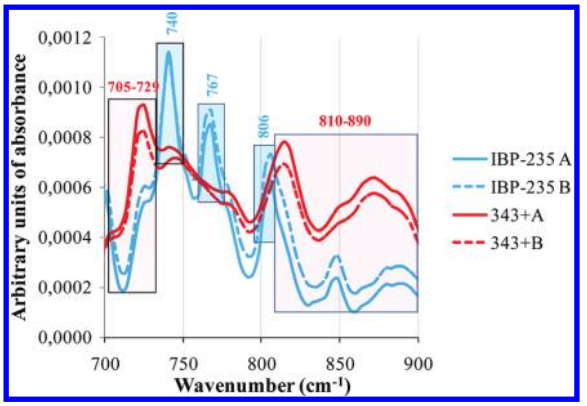

Figure 6. IR spectra of fractions from sequences A and B in the spectral region 700−900 cm^{-1}.

functions to simulate 11 bands in all the cases. The fitting of the aromatic region of sample 27 from sequence B is shown as an

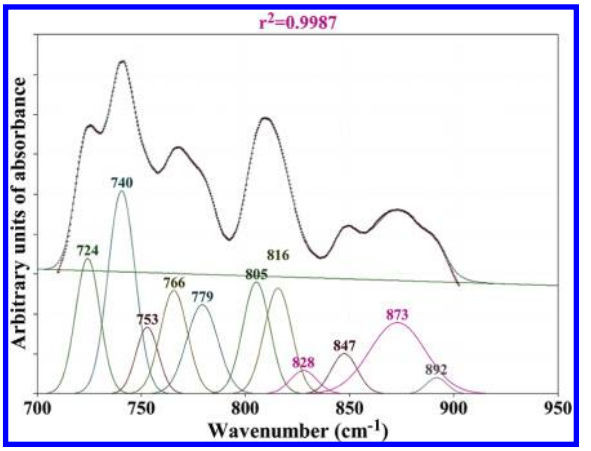

Figure 7. Deconvolution of region 700−900 cm^{-1} for sample 27 B.

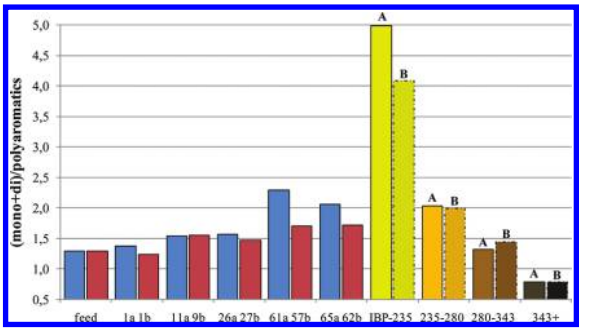

Figure 8. (Mono- + di-)/polyaromatics ratio for selected samples and distillation cuts from sequences A and B.

example in Figure 7. The ratios mono- plus di- over polyaromatics were calculated using eq 2, proposed in the present word (average determined maxima wavenumbers are included in the equation).

$$\left(\frac{\text{mono-} + \text{di-}}{\text{polyaromatics}}\right) = \left(\frac{A_{740} + A_{766} + A_{806}}{A_{816} + A_{870} + A_{890}}\right) \quad (2)$$

The samples, 61 A and 57 B, with highest conversion and lowest density among products had highest (mono- + di-)/polyaromatic relationship, as shown in Figure 8. As for distillation cuts, the expected dramatic increase of this parameter is evidenced when moving from 343+ °C fractions up to IBP−235 °C naphtha. Noteworthy, samples 61 A and 65 A had less aromatic condensation degree compared to their equivalent products (57 B and 62 B), also determined for the IBP−235 °C fraction A with respect to B. This could be related to different selectivity of the catalyst formulation toward mono- and diaromatic rings.

An inverse correlation between density and the (mono- + di-)/polyaromatic parameter was found. A nonlinear correlation for these two properties was found and is presented in Figure 9a. The higher density samples have a lower value for the (mono- + di-)/polyaromatic parameter, that is, a higher aromatic condensation degree.

Regarding aliphatic branches, during hydroprocessing, these chains are broken most commonly at the beta position from the rings, and hydrogen saturation of these broken bonds leads to methyl groups (CH_3) increasing at the expense of methylene

dx.doi.org/10.1021/ef201562j |*Energy Fuels* 2012, 26, 586–593

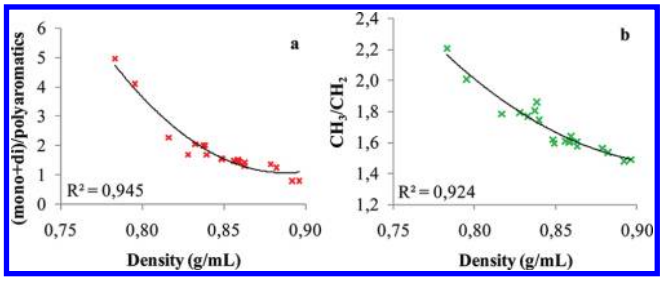

Figure 9. Correlation between density and (a) (mono- + di-)/polyaromatics (b) CH_3/CH_2.

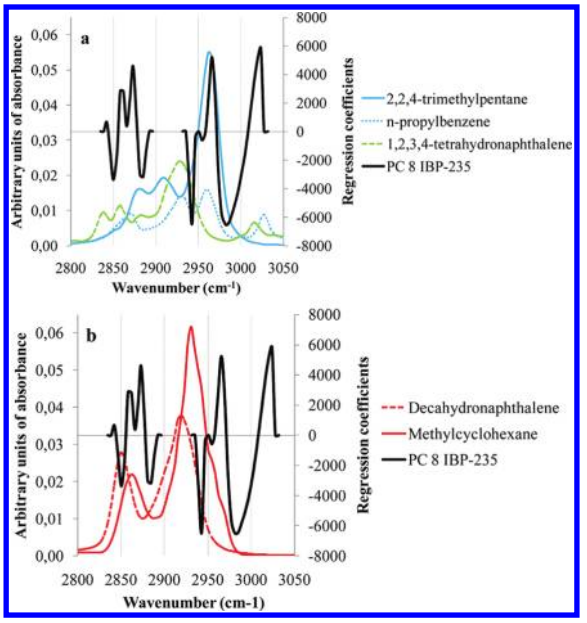

Figure 10. Comparison between IBP−235 model regression coefficients and IR spectra at the region 2800−3050 cm^{-1} of (a) mono- and diaromatic standard HCs and (b) polyaromatic standard HCs.

groups (CH_2). The increase in methyls and the decrease in methylenes were already detected by PLS-R. The CH_3 asymmetric and symmetric stretching vibrational modes located at ∼2954 and ∼2870 cm^{-1} had positive *B*-coefficients for the IBP−235 °C model. In fact, one standard HC (2,2,4-trimethylpentane), which has five CH_3 groups, showed its most intense band at 2966 cm^{-1} (see Figure 10a).

On the contrary, the CH_2 asymmetric and symmetric stretching vibrational modes usually assigned at ∼2920 and ∼2850 cm^{-1} had negative *B*-coefficients. Decahydronaphatelene and methylcyclohexane with eight and six CH_2 groups, respectively, have their most intense bands near 2920 and 2850 cm^{-1} (Figure 10b).

The former assignments are validated considering the relative intensities for IR spectra of distillation fractions from the two sets of experiments A and B. Figure 11 clearly shows that the bands at 2954 and 2870 cm^{-1} are more intense for the fraction IBP−235 °C, while in the fraction 343+ °C the band at 2854 cm^{-1} is more intense.

The positive value of *B*-coefficient for ∼3023 cm^{-1} could be associated with the C_{ar}−H bond of monoaromatic rings. Although the band at 3067−3058 cm^{-1} corresponding to the C_{ar}−H stretching mostly originates in the motion of the quarto hydrogens, specific vibrations arising from duo or solo hydrogens

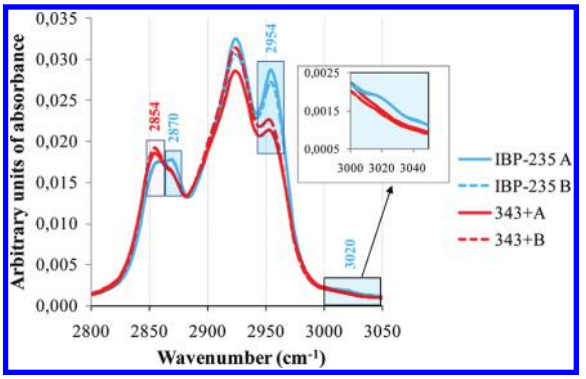

Figure 11. IR spectra of fractions from sequences A and B in the spectral region 2800−3050 cm^{-1}.

have been sorted out and do not show any special behavior.[22] However, *n*-propylbenzene and 1,2,3,4-tetrahydronaphtalene have a single band at ∼3020 cm^{-1}, unlike other aromatic compounds in which distinguishing a patron at the region 3000−3050 cm^{-1} was not possible. The IBP−235 °C fraction has a higher intensity than the 343+ °C cut around this wavenumber (see Figure 11). The ratio between the areas of bands centered in 2954 and 2854 cm^{-1} was calculated (eq 3).[25]

$$\left(\frac{CH_3}{CH_2}\right) = \left(\frac{A_{2954}}{A_{2854}}\right) \quad (3)$$

This was possible after deconvoluting the region from 2800 to 3050 cm^{-1} following a similar procedure, as described previously. This parameter is the relation between CH_3− and −CH_2− functional groups and is related to the aliphatic chain length. A nonlinear correlation of density and aliphatic chain length was found and presented in Figure 9b. According to this, a product with high density (low conversion) is enriched with long aliphatic chains and vice versa.

CONCLUSION

Seven validated models for predicting density, nitrogen and sulfur contents, and weight percentage of the distillation ranges IBP−235 °C, 235−280 °C, 280−343 °C, 343+ °C for hydroprocessed full gas oils were obtained through IR spectroscopy and PLS-R, using the procedure of reduction of variables published by Orrego-Ruiz et al.[15] Once the models were built, the time spent for prediction of all these properties is a fraction (about 1 h versus 1 day) of what it would span with traditional methods, indicating that this methodology is faster, cheaper, and suitable for monitoring purposes. Low errors of prediction support the reliability of the methodology for monitoring heavy distillates hydroprocessing. The *B*-coefficients for IBP−235 °C and 343+ °C models were used for detailed chemical understanding of full gas oils hydroprocessing. These coefficients and their variations in two IR spectral regions allowed proposing two structural parameters for detecting hydrocarbons redistributions, one of them (eq 2) unpublished until now. These ancillary parameters could complement the routine monitoring of upgrading processes, being possible through them to conclude that, in the studied case, polyaromatic rings were hydrogenated toward mono- and diaromatics and long alkyl substituents from large molecules were cracked into smaller compounds that partitioned into the pool of lighter distillates within products (IBP−343 °C). The IBP−235 °C fraction was determined to comprise mono- and

dx.doi.org/10.1021/ef201562j |*Energy Fuels* 2012, 26, 586–593

diaromatic rings, whereas the 343+ °C fraction preferentially contains polyaromatic rings.

AUTHOR INFORMATION

Corresponding Author
*Tel.: (57) 7 6344000 ext: 2247. E-mail: jorgecarbon2001@yahoo.es.

ACKNOWLEDGMENT

The authors are grateful to NSERC-NEXEN-AIEES Industrial Research Chair Catalysis for Bitumen Upgrading, Schulich School of Engineering University of Calgary for funding and to Colciencias for its Scholarship "Francisco José de Caldas" given to Jorge A. Orrego-Ruiz.

REFERENCES

(1) Rana, M. S.; Sámano, V.; Ancheyta, J.; Diaz, J. A. I. *Fuel* **2007**, *86*, 1216–1231.
(2) Loria, H.; Trujillo-Ferrer, G.; Sosa-Stull, C.; Pereira-Almao, P. *Energy Fuels* **2011**, *25*, 1364–1372.
(3) Speight, J. G. *Catal. Today* **2004**, *98*, 55–60.
(4) Speight, J. G. *The Chemistry and Technology of Petroleum*; CRC Press/Taylor & Francis: Boca Raton, FL, 2007.
(5) Lavine, B.; Workman, J. *Anal. Chem.* **2010**, *82*, 4699–4711.
(6) Gemperline, P. J. *Chemom. Intell. Lab. Syst.* **1992**, *15*, 115–126.
(7) Fernández-Varela, R.; Suárez-Rodríguez, D.; Gómez-Carracedo, M. P.; Andrade, J. M.; Fernández, E.; Muniategui, S.; Prada, D. *Talanta* **2005**, *68*, 116–125.
(8) McKelvy, M. L.; Britt, T. R.; Davis, B. L.; Gillie, J. K.; Lentz, L. A.; Leugers, A.; Nyquist, R. A.; Putzig, C. L. *Anal. Chem.* **1996**, *68*, 93R–160R.
(9) Trujillo-Ferrer, G. L. Thermal and Catalytic Steam Reactivity Evaluation of Athabasca Vacuum Gasoil, MSc Thesis, University of Calgary, Calgary, AB, Canada, 2008.
(10) Carbognani, L.; Lubkowitz, J.; Gonzalez, M. F.; Pereira-Almao, P. *Energy Fuels* **2007**, *21* (5), 2831–2839.
(11) Carbognani, L.; Carbognani-Arambarri, L.; López-Linares, F.; Pereira-Almao, P. *Energy Fuels* **2011**, *25*, 3663–3670.
(12) López-Linares, F.; Carbognani, L.; Spencer, R. J.; Pereira-Almao, P. *Energy Fuels* **2011**, *25*, 3657–3662.
(13) American Society for Testing and Materials (ASTM) International. *ASTM D2892-03a*, Standard Test Method for Distillation of Crude Petroleum (15-Theoretical Plate Column); ASTM International: West Conshohocken, PA, 2003.
(14) American Society for Testing and Materials (ASTM) International. *ASTM D 5236-03*, Standard Test Method for Distillation of Heavy Hydrocarbon Mixtures (Vacuum Pot Still Method); ASTM International: West Conshohocken, PA, 2003.
(15) Orrego-Ruiz, J. A.; Guzmán, A.; Molina, D.; Mejía-Ospino, E. *Energy Fuels* **2011**, *25*, 3678–3686.
(16) *The Unscrambler*, Version 10.1 User Manual; CAMO Software AS: Oslo, Norway, 2011.
(17) Martens, H.; Martens, M. *Food Qual. Preference* **2000**, *11*, 5–16.
(18) Chung, H.; Ku, M.; Lee, J. S. *Appl. Spectrosc.* **2000**, *54*, 239–245.
(19) Guillén, M. D.; Iglesias, M. J.; Dominguez, A.; Blanco, C. G. *Energy Fuels* **1992**, *6*, 518–525.
(20) Ibrahim, H. H.; Idem, R. O. *Energy Fuels* **2004**, *18*, 1354–1369.
(21) Álvarez, P.; Granda, M.; Sutil, J.; Menendez, R.; Fernandez, J. J.; Viña, J. A.; Morgan, T. J.; Millan, M.; Herod, A. A.; Kandiyoti, R. *Energy Fuels* **2008**, *22*, 4077–4086.
(22) Pauzat, F.; Ellinger, Y. *Chem. Phys.* **2002**, *280*, 267–282.
(23) Langhoff, S. R. *J. Phys. Chem.* **1996**, *100*, 2819–2841.
(24) Vala, M.; Szczepanski, J. *J. Phys. Chem.* **1994**, *98*, 9187–9196.
(25) Pironon, J.; Barres, O. *Geochim. Cosmochim. Acta* **1990**, *54* (3), 509–518.